Inorg. Chem. **2003**, *42*, 3779–3787

Induced Fit Process in the Selective Distal Binding of Imidazoles in Zinc(II) Porphyrin Receptors†

Dharam Paul,‡ Frédéric Melin,‡ Caroline Hirtz,‡ Jennifer Wytko,‡ Philippe Ochsenbein,§ Michel Bonin,|| Kurt Schenk,|| Patrick Maltese,⊥ and Jean Weiss*,‡

Laboratoire d'Electrochimie, UMR 7512 au CNRS, Université Louis Pasteur, 4 rue Blaise Pascal, F-67070 Strasbourg, France, Sanofi-Synthélabo, 371 rue du Prof. Blayac, F-34000 Montpellier, France, Département Sciences Physiques, Université de Lausanne, CH-1015 Lausanne-Dorigny, Switzerland, and Laboratoire de Chimie Supramoléculaire ISIS, Université Louis Pasteur, 4 rue Blaise Pascal, F-67070 Strasbourg, France

Received February 14, 2003

The respective affinities of various imidazole derivatives, imidazole (ImH), 2-methylimidazole (2-MeImH), 2-phenylimidazole (2-PhImH), *N*-methylimidazole (*N*-MeIm), 2-methylbenzimidazole (2-MeBzImH), and 4,5-dimethylbenzimidazole (4,5-Me_2BzImH), for two phenanthroline (Phen) strapped zinc(II) porphyrin receptors porphen–Zn **1**-Zn and **2**-Zn have been studied. The formation of a supplementary H-bond considerably enhances the affinity of the zinc(II)–porphen receptor for imidazoles unsubstituted on the pyrrolic nitrogen (ImH) versus N-substituted imidazoles such as *N*-MeIm. The ImHs⊂porphen–Zn complexes are formed with association constants up to 4 orders of magnitude superior to those measured either for *N*-MeIm as substrate or TPP–Zn as receptor. Distal or proximal binding of the substrates was determined by ^{1}H NMR measurements and titration. In two cases, the very high stability of the inclusion complex enabled the use of 2D NMR techniques. Excellent correlation between solution and solid-state structures has been obtained. A total of six X-ray structures are detailed in this article showing that the evolution of the shape of the zinc(II) receptor is mostly dependent on the steric constraints induced by the substitution on the imidazole. Hindered guests also progressively induce considerable mobility restrictions and severe distortions on the receptor, especially in the case of 2-MeBzImH and 2-PhImH.

Introduction

Ditopic ligands based on porphyrins are of great interest for modeling naturally occurring bimetallic active sites such as cytochrome *c* oxidase in which copper and hemic iron are involved in the fixation and the four electron reduction of molecular dioxygen.[1−5] Two main approaches have been developed that consist of either in situ forming of bridged copper(II) and iron(III) complexes,[6,7] for example starting from copper(I) and iron(II), or covalently linking a binding site for copper(II/I) to an iron porphyrin.[8] The latter approach has been widely used by the group of Collman to prepare functional analogues of heme protein active sites.[9] Due to their design, ditopic ligands built on porphyrins exhibit a structure/reactivity relationship similar to strapped, picket-

* To whom correspondence should be addressed. E-mail: jweiss@chimie.u-strasbg.fr.

† This article is dedicated to Dr. Christiane Dietrich-Buchecker on the occasion of her 61st birthday.

‡ Laboratoire d'Electrochimie, Université Louis Pasteur.
§ Sanofi-Synthélabo Recherche.
|| Département Sciences Physiques, Université de Lausanne.
⊥ Laboratoire de Chimie Supramoléculaire ISIS, Université Louis Pasteur.

(1) Scott, R. A. *Annu. Rev. Biophys. Chem.* **1989**, *18*, 137.
(2) Chan, S. I.; Li, P. M. *Biochemistry* **1990**, *29*, 1.
(3) Babcock, G. T.; Wilkström, M. *Nature* **1992**, *356*, 301.
(4) Malmström, B. G. *Acc. Chem. Res.* **1993**, *26*, 332.
(5) For characterization of different states of the enzyme, see: (a) Rich, P. R.; Breton, J. *Biochemistry* **2001**, *40*, 6441. Morgan, J. E.; Verkhovsky, M. I.; Palmer, G.; Wilkström, M. *Biochemistry* **2001**, *40*, 6882. Hagen, W. R. *Biochim. Biophys. Acta* **1982**, *708*, 82. (b) Dunham, W. R.; Sands, R. H.; Shaw, R. W.; Beinert, H. *Biochim. Biophys. Acta* **1983**, *748*, 73. (c) Hagen, W. R.; Dunham, W. R.; Sands, R. H.; Shaw, R. W.; Beinert, H. *Biochim. Biophys. Acta* **1984**, *765*, 399. (d) Blair, D. F.; Witt, S. N.; Chan, S. I. *J. Magn. Reson.* **1986**, *67*, 189. (e) Ogura, T.; Takahashi, S.; Shinzawa-Itoh, K.; Yoshikawa, S.; Kitagawa, T. *J. Am. Chem. Soc.* **1990**, *112*, 5630.
(6) (a) Lim, B. S.; Holm, R. H. *Inorg. Chem.* **1998**, *37*, 4898 and references cited. (b) Holm, R. H. *Pure Appl. Chem.* **1995**, *67*, 217.
(7) (a) Ghiladi, R. A.; Hatwell, K. R.; Karlin, K. D.; Huang, H.; Moënne-Loccoz, P.; Krebs, C.; Huynh, B. H.; Marzilli, L. A.; Cotter, R. J.; Kaderli, S.; Zuberbühler, A. D. *J. Am. Chem. Soc.* **2001**, *123*, 6183 and references cited. (b) Karlin, K. D.; Nanthakumar, A.; Fox, S.; Murthy, N. N.; Ravi, N.; Huynh, B. H.; Orosz, R. D.; Day, E. P. *J. Am. Chem. Soc.* **1994**, *116*, 4753 and references cited.

10.1021/ic0341643 CCC: $25.00
Published on Web 05/21/2003

fence, or "basket handle" porphyrins, namely the topographical control of axial base coordination, the presence of straps mimicking the distal site of natural hemoproteins while the open face of the porphyrin is considered as the proximal site.[10]

In Nature, the complementarity of numerous additive weak interactions is usually responsible for highly organized assemblies. The role of weak distal interactions (e.g. steric, electrostatic, H-bonding) is emphasized by the CO/O_2 discrimination in hemoproteins[11] and by the interest in hindered heme for the study of magnetic properties. Indeed, the combination of axial auxiliary binding on metalloporphyrins and peripheral interactions such as H-bonding or hydrophobic π-stacking has resulted in an elegant approach of modeling heme-dependent proteins.[12] The properties of iron porphyrins and 2-methylimidazole (2-MeImH) appear to be highly dependent on the position of the axial ligand which has been shown to be a determining factor for the catalytic properties of hemes.[13] A structure−property relationship study has established correlation between heme properties and 2-MeImH alignment in the case of cytochrome *c*, showing that axial base binding in heme proteins and related topographic changes are of major importance in the fine-tuning of heme properties.[13] Recent reports in the field of superstructured porphyrins have shown that axial ligand selection can be achieved by proper positioning of H-binding sites within the straps or the basket handles.[14] The recognition

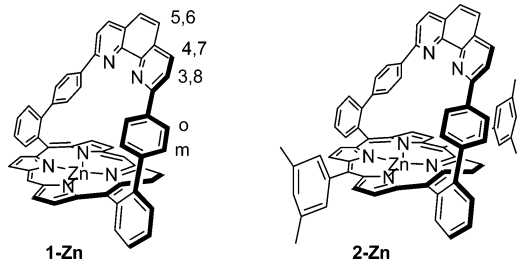

Figure 1. Two receptors used for the recognition of N-unsubstituted imidazoles.

of chiral amino acids demonstrates that the information learned from modeling heme proteins can be utilized as input into the design of selective receptors based on zinc(II) porphyrins.[7] On the basis of these considerations, the combination of strong direct interactions with the metallic core of a porphyrin and weak interactions located around the axial ligand(s) is more frequently utilized to control the selectivity of the axial ligation on zinc or iron porphyrins. Several recent papers have even outlined the importance of geometric changes that occur in hemoproteins upon ligand binding and its particular involvement regarding signal transduction.[15] Thus, topographic control of the axial base positioning and the geometrical changes resulting from this binding, are relevant to many metalloporphyrins properties.

We have previously described the synthesis of a highly rigid phenanthroline (Phen) strapped porphyrin **1** (porphen)[16] and its zinc complex **1**-Zn (Figure 1),[17] the use of this ligand to access copper and silver mixed-valence homobinuclear complexes,[18] and preliminary studies of axial base binding that have led to the unexpected formation of inclusion complexes with N-unsubstituted imidazoles.[19] On the basis of the same synthetic approach, a *meso*-substituted derivative

(8) For examples see: (a) Gunter, M. J.; Mander, L. N.; Murray, K. S.; Clark, P. E. *J. Am. Chem. Soc.* **1981**, *103*, 6784. (b) Chang, C. K.; Koo, M. S.; Ward, B. *J. Chem. Soc. Chem. Commun.* **1982**, 716. (c) Gunter, M. J.; Berry, K. J.; Murray, K. S. *J. Am. Chem. Soc.* **1984**, *106*, 4227. (d) Rodgers, S. J.; Koch, C. A.; Tate, J. R.; Reed, C. A., Eigenbrot, C. W.; Scheidt, W. R. *Inorg. Chem.* **1987**, *26*, 3647. (e) Bulach, V.; Mandon, D.; Weiss, R. *Angew. Chem., Int. Ed. Engl.* **1991**, *30*, 572. (f) Collman, J. P.; Herrmann, P. C.; Boitrel, B.; Zhang, X.; Eberspacher, T. A.; Fu, L.; Wang, J.; Rouseau, D. L.; Williams, E. R. *J. Am. Chem. Soc.* **1994**, *116*, 9783. (g) Bag, N.; Chern, S.-S.; Peng, S.-M.; Chang, C. K. *Inorg. Chem.* **1995**, *34*, 753. (h) Franceschi, F.; Gullotti, M.; Monzani, E.; Casella, L.; Papaefthymiou, V. *J. Chem. Soc., Chem. Commun.* **1996**, 1645.

(9) (a) Collman, J. P.; Fu, L.; Herrmann, P. C.; Wang, Z.; Broring, M.; Schwenninger, R.; Boitrel, B. *Angew. Chem., Int. Ed.* **1998**, *37*, 3397. (b) Collman, J. P.; Rapta, M.; Broring, M.; Raptova, L.; Boitrel, B.; Fu, L.; L'Her, M. *J. Am. Chem. Soc.* **1999**, *121*, 1387. (c) Rose, E.; Lecas, A.; Quelquejeu, M.; Kossyani, A.; Boitrel, B. *Coord. Chem. Rev.* **1998**, *180*, 1407 and references cited. (d) Collman, J. P. *Inorg. Chem.* **1997**, *36*, 5145 and references cited. (e) Collman J. P.; Eberspacher, T.; Fu, L.; Herrmann, P. C. *J. Mol. Catal., A* **1997**, *117* (1−3), 9. (f) Collman, J. P.; Fu, L.; Herrmann, P. C.; Zhang, X. M. *Science* **1997**, *275*, 949.

(10) (a) Collman, J. P.; Fu, L. *Acc. Chem. Res.* **1999**, *32*, 455. (b) Collman, J. P.; Herrmann, P. C.; Fu, L.; Eberspacher, T. A.; Eubanks, M.; Boitrel, B.; Hayoz, P.; Zhang, X.; Brauman, J. I.; Day, V. W. *J. Am. Chem. Soc.* **1997**, *119*, 3481. (c) Momenteau, M. Models of Hemoprotein Active Sites. In *Supramolecular Control of Structure and Reactivity*; Hamilton, A., Ed.; Wiley: New York, 1996; p 155. (d) Momenteau, M.; Reed, C. A. *Chem. Rev.* **1994**, *94*, 659.

(11) (a) Spiro, T. G.; Kozlowski, P. M. *J. Am. Chem. Soc.* **1998**, *120*, 4524 and references therein. (b) Slebodnick, C.; Ibers, J. A. *J. Biol. Inorg. Chem.* **1997**, *2*, 521. Gosh, A.; Bocian, D. F. *J. Phys. Chem.* **1996**, *100*, 6363. (c) Tétreau, C.; Lavalette, D.; Momenteau, M.; Fischer, J.; Weiss, R. *Biophys. J.* **1994**, *66*, 262. (d) Rose, E.; Boitrel, B.; Quelquejeu, M.; Kossyani, A. *Tetrahedron Lett.* **1993**, *34*, 7267. (e) Tétreau, C.; Momenteau, M.; Lavalette, D. *Inorg. Chem.* **1990**, *29*, 1727. (f) Traylor, T. G.; Koga, N.; Dearduff, J. A. *J. Am. Chem. Soc.* **1985**, *107*, 6504.

(12) Kuroda, Y.; Kato, Y.; Higashioji, T.; Hasegawa, J.; Kawanami, S.; Takahashi, M.; Shiraishi, N.; Tanabe, K.; Ogoshi, H. *J. Am. Chem. Soc.* **1995**, *117*, 10950.

(13) (a) Yao, Y.; Qian, C.; Wu, Y.; Hu, J.; Tang, W. *J. Chem. Soc., Dalton Trans.* **2001**, 1841 and reference cited. (b) Casella, L.; Monzani, E.; Fantucci, P.; Gullotti, M.; De Gioia, L.; Strini, A.; Chillemi, F. *Inorg. Chem.* **1996**, *35*, 439 and references therein. (c) Munro, O. Q.; Marques, H. M. *Inorg. Chem.* **1996**, *35*, 3752. (d) Nakamura, M.; Ikeue, T.; Neya, S.; Funasaki, N.; Nakamura, N. *Inorg. Chem.* **1996**, *35*, 3731. (e) Uno, T.; Hatano, K.; Nishimura, Y. *J. Am. Chem. Soc.* **1994**, *116*, 4107. (f) Nakamura, M.; Tajima, K.; Tada, K.; Ishizu, K.; Nakamura, N. *Inorg. Chim. Acta* **1994**, *224*, 113. (g) Walker, F. A.; Simonis, U. *J. Am. Chem. Soc.* **1991**, *113*, 8652. (h) Hatano, K.; Safo, M. K.; Walker, F. A.; Scheidt, W. R. *Inorg. Chem.* **1991**, *30*, 1643. (i) Nakamura, M.; Nakamura, N. *Chem. Lett.* **1991**, 1885. (j) Zhang, H.; Simonis, U.; Walker, F. A. *J. Am. Chem. Soc.* **1990**, *112*, 6124. (k) Nakamura, M.; Groves, J. T. *Tetrahedron* **1988**, *44*, 3225. (l) Rohmer, M. M.; Strich, A.; Veillard, A.; *Theor. Chim. Acta* **1984**, *65*, 219. (m) Traylor, T. G.; Berzinis, A. P. *J. Am. Chem. Soc.* **1980**, *102*, 2845.

(14) For recent reviews on molecular recognition involving zinc(II)−porphyrins, see: (a) Ogoshi, H.; Mizutani, T.; Hayashi, T.; Kuroda, Y. In *The Porphyrin Handbook*; Kadish, K. M., Smith, K. M., Guilard, R., Eds.; Academic Press: New York, 2000; Vol. 6, p 1. (b) Weiss, J. *J. Inclusion Phenom. Macrocyclic Chem.* **2001**, *40*, 1. (c) Middel, O.; Verboom, W.; Reinhoudt, D. N. *J. Org. Chem.* **2001**, *66*, 3998.

(15) (a) Haruta, N.; Aki, M.; Ozaki, S.; Watanabe, Y.; Kitagawa, T. I. *Biochemistry* **2001**, *40*, 6956 and references cited. (b) Trent, J. T., III; Hvitved, A. N.; Hargrove, M. S. *Biochemistry* **2001**, *40*, 6155. (c) Perry, C. B.; Chick, T.; Ntlokwana, A.; Davies, G.; Marques, H. M. *J. Chem. Soc., Dalton Trans.* **2002**, 449. (d) Ellison, M. K.; Schulz, C. E. Scheidt, W. R. *Inorg. Chem.* **2002**, *41*, 2173.

(16) Wytko, J. A.; Graf, E.; Weiss, J. *J. Org. Chem.* **1992**, *57*, 1015.

(17) Ochsenbein, P.; Bonin, M.; Schenk, K.; Froidevaux, J.; Wytko, J.; Graf, E.; Weiss, J. *Eur. J. Inorg. Chem.* **1999**, *2*, 1175.

(18) Giraudeau, A.; Gisselbrecht, J. P.; Gross, M.; Weiss, J. *J. Chem. Soc., Chem. Commun.* **1993**, 1103.

Scheme 1[a]

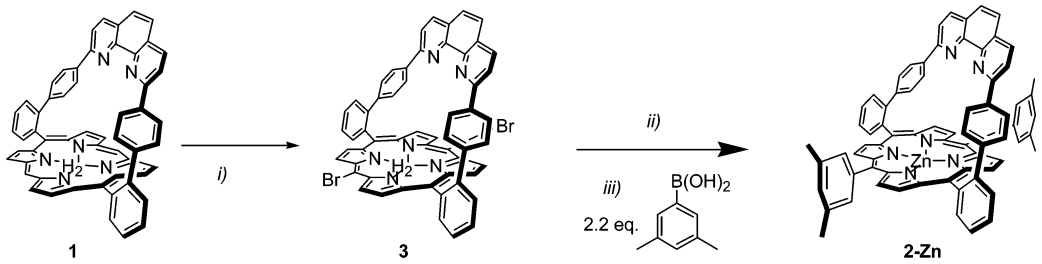

[a] Key: (i) NBS (2 equiv), pyridine, 0 °C, $CHCl_3$, 30 min, 69%; (ii) $Zn(AcO)_2$, THF, 30 min, 99%; (iii) 9% mol $Pd(PPh_3)_4$ (vs $R-B(OH)_2$), 2 M Na_2CO_3(aq) /MeOH/toluene (1:1:10), 80%.

2-Zn (Figure 1) has been prepared, bearing 3,5-dimethylphenyl or 5-*m*-xylyl substituents in two *meso* positions. This paper describes how, for these metalloporphyrins, the presence of the phenanthroline strap allows for both the selective distal or proximal coordination of axial imidazole derivatives and for the enhanced binding of N-unsubstituted imidazole (ImH). The topographic adjustments occurring in these receptors to accommodate various substrates will be detailed. Binding studies have been performed on receptors **1**-Zn and **2**-Zn with imidazole (ImH), 2-methylimidazole (2-MeImH), 2-phenylimidazole (2-PhImH), 2-methylbenzimidazole (2-MeBzImH), 4,5-dimethylbenzimidazole (4,5-Me_2BzImH), and *N*-methylimidazole (*N*-MeIm) using ^{1}H NMR and UV−visible titrations. Several zinc−porphyrin imidazole inclusion complexes have been characterized by single-crystal X-ray diffraction, and the changes of shape observed in the receptors due to substrate binding will be discussed. A highly distorted porphyrin ring is obtained upon coordination of 2-MeBzImH in **2**-Zn, providing a remarkable example of a distorted β-unsubstituted porphyrin.

Results and Discussion

Derivatization of Porphen 1. An advantage of the synthesis leading to porphyrin **1** is the large scale (up to gram quantities) on which this strapped porphyrin can be prepared.[16] Thus, this phenanthroline-strapped porphyrin may be considered as a starting material for more elaborate architectures. In this study, substitution of the remaining free *meso* positions has been achieved in two steps, beginning with NBS bromination of the unsubstituted *meso* positions in chloroform. Treatment of **1** with excess NBS afforded the dibromide **3** in 69% yield. As indicated in Scheme 1, metalation with zinc acetate in THF afforded a protection of the porphyrin core and enabled a clean coupling reaction involving the dibromide **3**-Zn and the *m*-xylylboronic acid[20] in classical Suzuki conditions to give the receptor **2**-Zn in 80% yield (see Supporting Information for details). Attempts to prepare the free base derivative **2**-H_2 from the dialdehyde precursor previously involved in the synthesis of **1** and a *m*-xylyldipyrrylmethane have resulted in poor isolated yields of porphyrin.

Table 1. log K_a of Axial Ligands with TPP−Zn, **1**-Zn, and **2**-Zn in CH_2Cl_2

receptor	substrate	pK_a[a] (substrate)	log K_{assn}	Soret[b]	Q bands[b]	Phen[b]
TPP−Zn	ImH	6.65	4.8 ± 0.2	428	562, 604	
TPP−Zn	*N*-MeIm	7.33	5.3 ± 0.2	428	564, 604	
TPP−Zn	2-MeImH	7.56	5.4 ± 0.2	428	564, 604	
1-Zn	ImH	6.65	6.1 ± 0.2	428	560, 598	284, 310
1-Zn	*N*-MeIm	7.33	4.7 ± 0.1	424	556, 592	286, 308
1-Zn	2-MeImH	7.56	7.3 ± 0.3	428	560, 596	284, 308
1-Zn	2-PhImH	7.50	6.4 ± 0.3	422	552	284, 310
2-Zn	ImH	6.65	5.9 ± 0.3	440	575, 616	283, 311
2-Zn	*N*-MeIm	7.33	3.3 ± 0.2	437	571, 611	285
2-Zn	2-MeImH	7.56	6.6 ± 0.3	440	575, 615	283, 309
2-Zn	2-PhImH	7.50	4.4 ± 0.3	441	576, 617	283, 309
2-Zn	2-MeBzImH	6.4	5.7 ± 0.2	441	573, 614	283, 309

[a] pK_a value obtained from the literature.[24] [b] λ_{max} in nm. Standard concentrations used: [substrate] = 2×10^{-2} M and [**1**-Zn] = [**2**-Zn] = 3×10^{-6} and 4×10^{-5} M for determination of log K_a from Soret bands and Q-bands, respectively.

As preliminary studies for the paramagnetic iron(II) complexes, the affinities of the two diamagnetic zinc(II) receptors **1**-Zn and **2**-Zn for a variety of imidazoles have been studied to estimate their ability to form pentacoordinated complexes of a divalent metal. The results obtained have focused our attention on the unique binding properties of this series of phenanthroline-strapped porphyrins.

UV−Visible Titrations and Stability Constants. In this study, Job plots obtained from UV−visible titrations of receptors **1**-Zn or **2**-Zn with various imidazoles have confirmed a 1:1 stoichiometry in each case, and thus, for all titrations performed,[21] data have been analyzed considering a pentacoordinated zinc(II) atom. Except for a few examples, in which in the solid state the zinc(II) has been shown to be hexacoordinated,[22] axial ligation of N-donor ligands usually affords pentacoordinated zinc(II) ions.[23] The results of UV−visible titrations in CH_2Cl_2 are collected in Table 1.

For comparison, association constants of ImH, *N*-MeIm, and 2-MeImH with (*meso*-tetraphenylporphyrinato)zinc(II), TPP−Zn, used as a reference, have been determined or collected from literature (see Table 1).

Spectral changes observed during the coordination of axial auxiliary ligands on zinc(II) porphyrins have been exhaus-

(19) Froidevaux, J.; Ochsenbein, P.; Bonin, M.; Schenk, K.; Maltese, P.; Gisselbrecht, J.-P.; Weiss, J. *J. Am. Chem. Soc.* **1997**, *119*, 12362.
(20) Schmid, M.; Eberhardt, R.; Klinga, M.; Leskela, M.; Rieger, B. *Organometallics* **2001**, *20*, 2321.
(21) For the titration method and treatment of the data, see: (a) Kirskey, C. H.; Hambright, P. Storm, C. B. *Inorg. Chem.* **1969**, *10*, 2141. (b) Anzai, K.; Hosokawa, T.; Hatano, K. *Chem. Pharm. Bull.* **1986**, *34*, 1865.
(22) For examples of hexacoordination, see: Scheidt, W. R.; Eigenbrodt, C. W.; Ogiso, M.; Hatano, K. *Bull. Chem. Soc. Jpn.* **1987**, *60*, 3529.
(23) For a compilation of Zn−N distances, see: Cheng, B.; Scheidt, W. R. *Inorg. Chim. Acta* **1995**, *237*, 5.

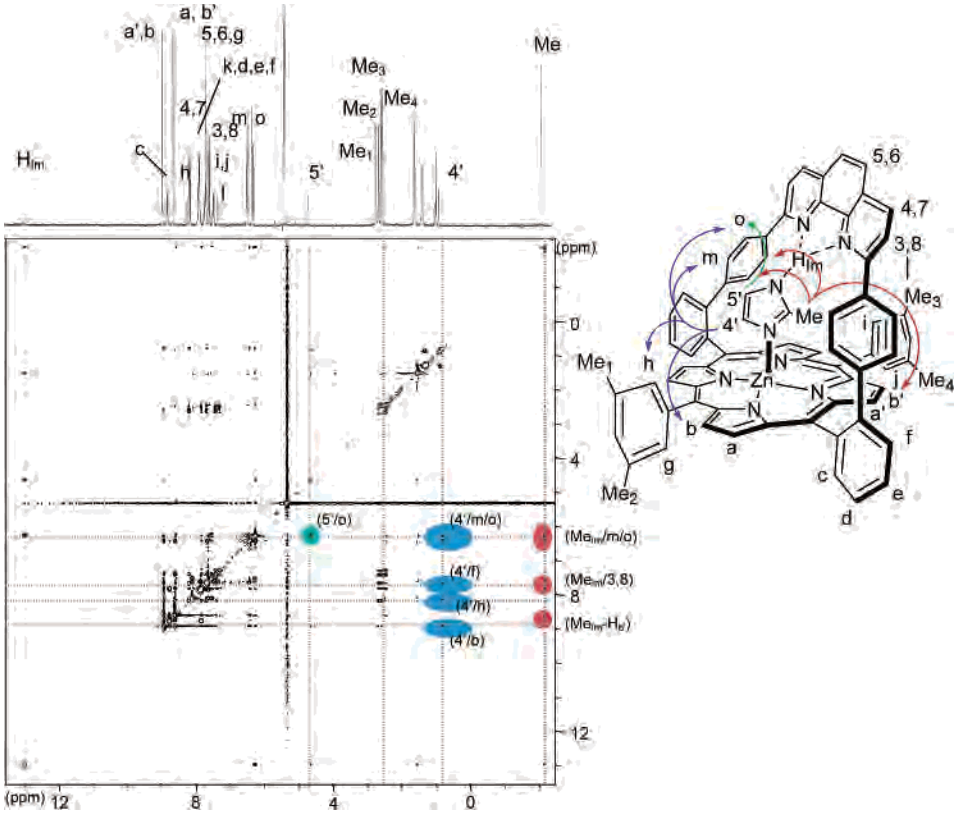

Figure 2. 2D ^{1}H NMR NOESY of the inclusion complex 2-MeImH⊂**1**-Zn, 300 MHz. $CHDCl_2$ (5.30 ppm) and trace of hexane (triplet at 0.90 ppm and broad signal at 1.3 ppm) from crystallization are present, together with residual water (singlet at 1.5 ppm).

tively analyzed in the literature, and the bathochromic shifts of the Soret and Q-bands observed in the pentacoordinated complexes of **1**-Zn and **2**-Zn are consistent with previously described results.[23]

Titration experiments have shown that from 0 to 1 equiv of substrate, in the case of N-unsubstituted imidazoles, not only the Soret and the Q-bands are affected by the coordination of the imidazole but also the Phen bands in the UV region of the spectrum. Similar experiments performed either with TPP−Zn as receptor or with *N*-MeIm and pyridine as substrates show no changes in the visible region of the spectra, neither from 0 to 1 equiv nor in the presence of slight excesses of the substrates. When huge excesses (averaging 80 equiv) of *N*-MeIm or pyridine are added, the typical red shifts of both the Soret band and the Q-band are observed.

Prior to further investigation of this phenomenon, the stability constants for each substrate with **1**-Zn or **2**-Zn and for a reference receptor TPP−Zn were calculated on the basis of titration experiments (Table 1). As a consequence of increasing pK_a values, the stability constants usually observed with zinc(II) porphyrins follow the order ImH < *N*-MeIm < 2-MeImH. For our receptors **1**-Zn and **2**-Zn, the higher association constants for ImHs in comparison with that obtained for *N*-MeIm clearly indicate that additional interactions must occur during their binding. As shown in Table 1, the presence of a hindered strap typically reduces the statistical approach of the axial base to only one side of the porphyrin. In the case of **1**-Zn and **2**-Zn, the presence of the Phen strap introduces a discrepancy in the binding strength series, *N*-MeIm ≪ ImH ≪ 2-MeImH, as well as a drastic enhancement of the stability constants exhibited with protic imidazoles. The reason for this enhancement obviously involves the phenanthroline moiety, as intensity changes in the phenanthroline absorption bands (284 and 310 nm) were observed during all titrations with ImHs. Evidence for H-bonding of the ImHs to the Phen nitrogens has been obtained from ^{1}H NMR data (see Supporting Information) and confirmed by both 2D ^{1}H NMR and single-crystal X-ray diffraction.

2D ^{1}H NMR Studies. 2D NMR experiments could be performed due to the high stability of 2-MeImH complexes with the two receptors **1**-Zn (ROESY) and **2**-Zn (NOESY). These experiments allowed unambiguous peak assignments and correlate exceptionally well with the corresponding solid-state structures (vide infra). Fully assigned ROESY plots for 2-MeImH⊂**1**-Zn are provided as Supporting Information, as they confirm previous assignments obtained by selective irradiations in NOEMULT.[19] For 2-MeImH⊂**2**-Zn, Figure 2 depicts highly significant correlations observed in the region comprised between the H_{ImMe} resonance at $\delta = -2.15$ ppm and the H_{ImN-H} signal at $\delta = 13.05$ ppm. The large chemical shift range covered by this plot has primarily allowed the assignment of correlations among imidazole $H_{Im5'}$, $H_{Im4'}$, and H_{ImMe} protons and neighboring protons on **2**-Zn (expanded NOESY from 2 to 9 ppm is available as Supporting Information). In particular, correlation of $H_{Im4'}$ with H_m, H_o, H_h, and H_b confirms, first of all, the location of the imidazole plane between the spacers and the proximity of its C=C bond with one of the xylyl groups and, second,

Table 2. Crystallographic Data for Inclusion Complexes 2-PhImH⊂**1**-Zn, 2-MeImH⊂**2**-Zn, 2-MeBzImH⊂**2**-Zn, and 2-PhImH⊂**2**-Zn

param	2-PhImH⊂**1**-Zn	2-MeImH⊂**2**-Zn	2-MeBzImH⊂**2**-Zn	2-PhImH⊂**2**-Zn
empirical formula	$C_{65}H_{40}N_8Zn$	$C_{100}H_{85}N_8Zn$	$C_{81.4}H_{59.1}Cl_2N_8$ Zn	$C_{84}H_{62}Cl_6N_8Zn$
fw	998.42	1464.13	1286.16	1461.49
crystal system	orthorhombic	monoclinic	monoclinic	monoclinic
lattice params				
a (Å)	21.453(4)	25.060(5)	14.859(3)	13.441(3)
b (Å)	11.001(2)	13.692(5)	18.671(4)	22.398(5)
c (Å)	20.066(4)	23.533(5)	24.067(5)	24.133(5)
β (deg)		101.551(5)	93.10(3)	100.80(3)
V (Å^3)	4735.3(16)	7911(4)	6667(2)	7137(2)
space group	Pnam	$P2_1/c$	$P2_1/n$	$P2_1/c$
Z (no. of molecules/unit cell)	4	4	4	4
D(calcd) (g cm^{-3})	1.400	1.229	1.281	1.360
μ(Mo Kα) (cm^{-1})	5.73	3.65	5.01	6.22
data collcn temp (°C)	−30	−113	−113	−93
$2\theta_{max}$ (deg)	56.22	48.06	48	51.94
no. of observns used ($I > 2\sigma(I)$)	5879	8656	6935	9228
no. of variables	373	1054	885	995
max shift/error on last LS cycle	0.051	0.002	0.084	−0.622
goodness of fit (GoF)[a]	0.924	1.136	0.982	0.920
resids:[a] R_1; wR_2	0.0492; 0.0943	0.0554; 0.1553	0.0451; 0.1232	0.0549; 0.1376
abs corr	none	none	none	none
largest peak in last diff map (e Å^{-3})	0.259	0.664	0.348	0.792

[a] $GoF = \{\sum[w(F_o^2 - F_c^2)^2]/(N_{ref} - N_{var})\}^{1/2}$; $R_1 = \sum||F_o| - |F_c||/\sum|F_o|$; $wR_2 = \{\sum[w(F_o^2 - F_c^2)^2]/\sum[w(F_o^2)]^2\}^{1/2}$.

allows an unambiguous assignment of the H_b resonance. Located further above the porphyrin ring, $H_{Im5'}$ is in spatial contact only with H_o and not with H_m. The correlation of H_{ImMe} with H_o and H_m confirms that the phenyl spacers are freely rotating but that the imidazole is fixed in the cavity, H_{ImMe} correlating with H_k and $H_{b'/a}$, as well as with H_{Me3}. All correlation assignments have been made using the H_{MeIm}/H_k, $H_{4'Im}/H_b$, and $H_{4'Im}/H_h$ correlations as a starting point.

Despite the fact that 2-MeBzImH is tightly bound in the cavity of **2**-Zn, it was not possible to perform 2D NMR experiments due to the extreme broadening of the spectrum. In the case of 2-PhImH, complexation within the cavity is clearly indicated by the chemical shifts displacements of H_o and H_m, but a weaker complexation is observed in a slowly exchanged inclusion complex.

X-ray Diffraction Studies. Six crystallographic structures of inclusion complexes with receptors **1**-Zn and **2**-Zn have been obtained. Although structures of ImH⊂**1**-Zn, and 2-MeImH⊂**1**-Zn have already been briefly described,[17] structural features concerning these complexes will be used for comparison throughout this discussion. Single crystals were obtained by slow diffusion of hexane in 1:1 mixtures of receptors and substrates in CH_2Cl_2, except for 2-PhImH and **2**-Zn for which a 10-fold excess of the substrate was used (Table 2). All crystals were air stable except for complexes of 2-MeBzImH⊂**2**-Zn and 2-PhImH⊂**2**-Zn, which required handling in mineral oil in an open glass capillary. It should be noted that in the case of 2-MeBzImH⊂**2**-Zn, 2-PhImH⊂**1**-Zn, and 2-PhImH⊂**2**-Zn, solution studies did not show full binding of the substrate for equimolar mixtures of substrate and receptor. Despite many attempts, crystallization of the complexes resulting from proximal coordination with *N*-alkylimidazoles has never led to single crystals.[17]

As a general feature, all the coordination complexes display distal inclusion of the imidazole guests. In each structure, the pyrrolic proton of the imidazole guest (H82) has been located by the presence of residual electronic density. The distances measured between H82 and the Phen nitrogen atoms N42 and N45 vary from 1.87 to 2.61 Å (Table 3), confirming the presence of a strong bifurcated hydrogen bond.

Table 3. Distances between Imidazole N−H (H82) and the Phen Nitrogen Atoms (N42, N45)[a]

complex	H82−N42	H82−N45
2-PhImH⊂**2**-Zn	2.034	2.260
2-MeImH⊂**2**-Zn	2.075	2.426
2-MeBzImH⊂**2**-Zn	1.868	2.606
2-PhImH⊂**1**-Zn	2.185	2.185

[a] Distances in Å.

A ruffling of the tetrapyrrolic macrocycle is generally observed upon coordination of the guest to the central zinc atom, and all the structures present a more or less pronounced tilt of the Phen strap over the porphyrin ring. This tilt (65°) was previously observed in the free base crystallographic structure and was assigned to packing interactions. For ImHs inclusion complexes, several factors contribute to reduce or enhance the degree of tilting.

When compared with structures of ImH⊂**1**-Zn and 2-MeImH⊂**1**-Zn, the structure of 2-PhImH⊂**1**-Zn (Figure 3) shows additional distortion of the porphyrin macrocycle to accommodate the aromatic substituent of the imidazole guest. The Phen plane is brought closer to the normal to the porphyrin plane, reducing the tilt of the strap above the porphyrin plane (dihedral angle 78.1°) and forcing the Zn−N_{Im} bond to deviate 8.9° from the normal to the porphyrin plane.

These small changes induced by steric constraints also allow additional stabilizing interactions to be developed between the phenyl ring of the imidazole and the porphyrin core. The mean distance of 3.55(3) Å between the nearly parallel planes (2.2° dihedral angle) of the porphyrin nucleus and the phenyl substituent of the substrate is perfectly adequate for efficient $\pi-\pi$ interactions. In addition, an offset, positioning the *meso* carbon of the porphyrin on the normal

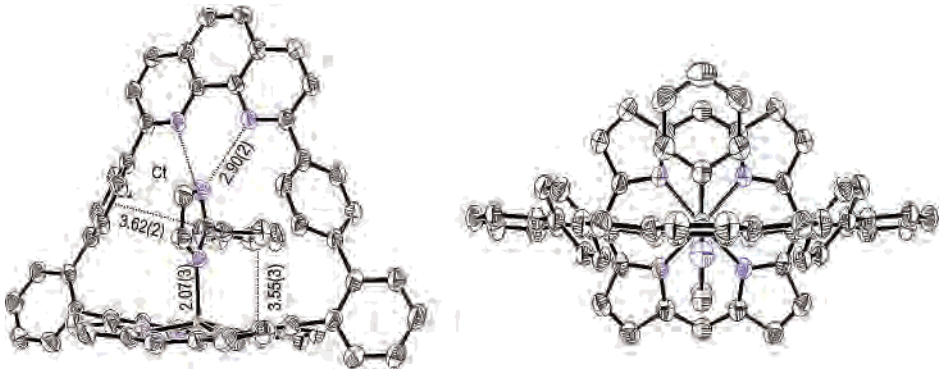

Figure 3. Front (left) and top view (right) of 2-PhImH⊂**1**-Zn displaying relevant distances discussed in the text. Ct is an artificially generated centroid on the phenyl spacer.

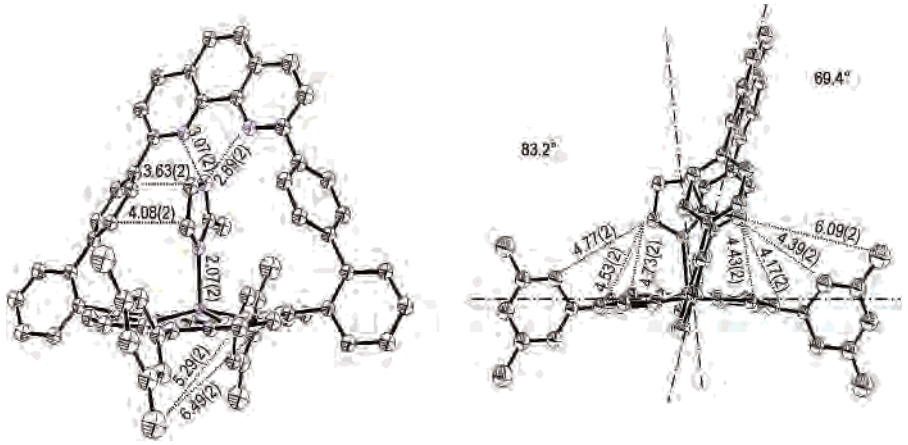

Figure 4. Front view (left) and side view (right) of the 2-MeImH⊂**2**-Zn inclusion complex. Significant distances and angles discussed in text are represented.

Table 4. Projection of Zn−N_{Im} and N_{Phen}−NH_{Im} Distances, along the N_{Phen}−Zn Axis, in the Solid-State Structures in **1**-Zn and **2**-Zn Inclusion Complexes with Various Imidazole Substrates and Evaluation of the Space Left for Imidazole Binding[a]

no.	Param	ImH⊂**1**-Zn[b]	2-MeImH⊂**1**-Zn[b]	2-PhImH⊂**1**-Zn[c]	2-MeImH⊂**2**-Zn[c]	2-MeBzImH⊂**2**-Zn[c]	2-PhImH⊂**2**-Zn[c]
1	Zn−N_{Im}	1.9	1.9	1.9	1.9	1.9	1.9
2	N_{Im}–N_{Phen}(av)	2.8	2.6	2.6	2.7	2.7	2.7
3	tot. **1** + **2**	4.7	4.5	4.5	4.6	4.6	4.6
4	Zn−N_{Phen}(av)	6.4	6.7	6.8	6.6	6.8	6.7
5	approximated space left (4 − 3)	1.7	2.2	2.3	2.0	2.2	2.1

[a] N---N distance in free imidazole ca. 2.2 Å. [b] Reference 19. [c] This work.

to the phenyl plane of the 2-PhImH guest, is observed as shown in Figure 3 (right). Two aromatic H atoms of this phenyl substituent also develop stabilizing interactions with the phenyl spacers that separate the phenanthroline and the porphyrin; the two phenyl protons H_2 and H_6 on the substrate point toward the center of the π cloud of each phenyl spacer of **1**-Zn. The distance between the centroid of the phenyl spacer and the phenyl C_2 atom of the 2-PhImH substrate bearing the hydrogen is quite short (3.62(2) Å) suggesting that strong CH---π interactions are established, at least in the solid state.[26]

Despite the 8.9° angle of the zinc−nitrogen bond with the normal to the mean plane of the porphyrin, the 2.07(3) Å distance between the pyridinic nitrogen of the imidazole and the zinc cation is comparable with literature data,[21] as is the distance of 2.89(2) Å between a Schiff base nitrogen atom of the phenanthroline and the imidazole pyrrolic N.[25]

The crystal structure of 2-MeImH⊂**2**-Zn (Figure 4) when compared to 2D ^{1}H NMR data is extremely representative of its solution structure. Additional information is provided by the distances of 3.07(2) and 2.89(2) Å between the pyrrolic nitrogen of the imidazole and the phenanthroline nitrogens. These distances are consistent with a strong, bifurcated hydrogen bond. Significant N_{Phen}−$NH_{imidazole}$ distances relevant to the binding strength are collected in Table 4. The 2.07(2) Å distance between the zinc(II) atom and the pyridinic nitrogen of the imidazole shows that the strength of the coordination bond is unaffected by substitution either of the substrate or of the porphyrin periphery. Contrary to rough predictions made from CPK models, our results clearly establish that the xylyl substituents are not bulky enough to inhibit the "distal" binding of the imidazole.

(24) Kadish, K. M.; Shive, L. R.; Bottomley, L. A. *Inorg. Chem.* **1981**, *20*, 1274.
(25) Steiner, T.; Desiraju, G. R. *J. Chem. Soc., Chem. Commun.* **1998**, 891.
(26) For discussion, see: Desiraju, G. R. *Acc. Chem. Res.* **2002**, *35*, 565 and references cited. For a database survey, see: Umezawa, Y.; Tsuboyama, S.; Takahashi, H.; Uzawa, J.; Nishio, M. *Tetrahedron* **1999**, *55*, 10047. For recent examples, see: Yamakawa, M.; Yamada, I.; Noyori, R. *Angew. Chem., Int. Ed. Engl.* **2001**, *40*, 2818.

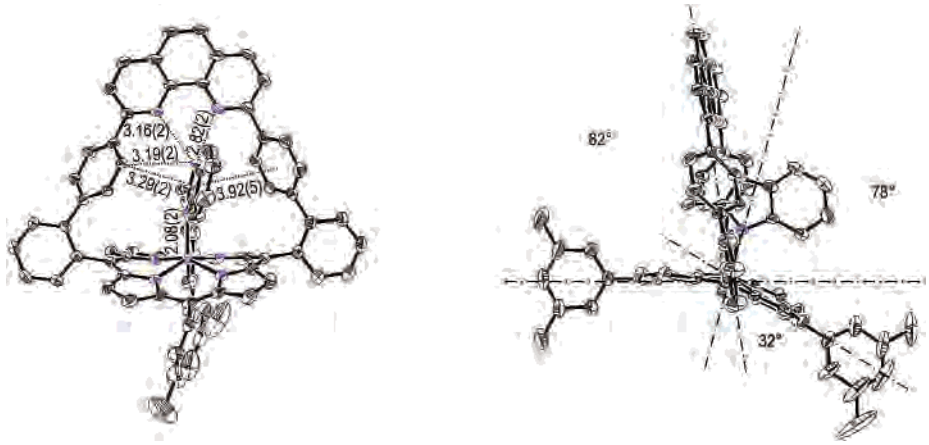

Figure 5. Front view (left) and side view (right) of the distorted 2-MeBzImH⊂**2**-Zn inclusion complex. A side view shows the puckered porphyrin ring and the deviated zinc−N bond.

Even more surprising has been the success in crystallizing the 2-MeBzImH complex (vide infra), which was unexpected considering the lower association constant (Table 1). In the case of 2-methyl-substituted imidazoles, CH−π interactions may further contribute to the stabilization of the inclusion complexes. In the structure of 2-MeImH⊂**2**-Zn, the hydrogen atoms (H84a−c) of the methyl substituent (2-MeIm) have been located by X-ray diffraction. Two of these hydrogen atoms (H84a,b) are pointing toward the porphyrin ring while the third (H84c) is pointing upward in the direction of the Phen nucleus. H84a,b are respectively located at 3.00 and 2.83 Å from the aromatic porphyrinic nitrogen atoms N24 and N21 and 3.26 and 2.92 Å from the center of the pyrrolic rings containing N24 and N21. H84c interacts with the aromatic phen nitrogen atoms N42 and N45 at distances of 2.86 and 2.93 Å. Both distances are consistent with rather strong CH−π interactions according to literature data.[26]

The molecular structure of 2-MeBzImH⊂**2**-Zn shown in Figure 5 provides evidence for the tremendous flexibility of the receptor, as considerable geometric changes are observed in the framework.

Two types of distortions arise from inclusion of the benzimidazole substrate, one affecting the strap through rotations around the four single bonds connecting the tetrapyrrolic core with the Phen nucleus via the *meso* phenyl substituents and the other concerning the porphyrin ring itself. The phenyl spacer on the left-hand side of the strap (Figure 5) is rotated to allow CH−N interactions in the solid state, between the H_o proton and the imidazole pyrrolic nitrogen (d = 3.19(2) Å), and CH−π interactions with the imidazole N_3═C_2 double bond (3.29(2) Å). The other phenyl spacer, on the right-hand side, is rotated so that it weakly stacks with the substrate, which is also slightly tilted in the cavity defined by the strap. The bifurcated H-bond is again unsymmetrical (3.16(2) and 2.82(2) Å) but still strong, and the plane of the porphyrin is puckered along the anchoring point of the strap to accommodate the steric hindrance of the benzimidazole. The Zn−N bond deviation from the normal to the plane defined by the four porphyrin nitrogen atoms is small and the axial coordination still strong with a bond length of 2.08(2) Å. Although the distortions affecting the strap are observed for other substrates, the amplitude of the changes is greater in the case of 2-MeBzImH because of the extended aromatic character of the guest. In fact, all distortions tend to maximize stabilizing $\pi-\pi$ and CH−π interactions without weakening the driving forces of the distal binding i.e. the Zn−N coordination bond and the bifurcated H-bond. These two interactions remain almost unchanged in their bond lengths throughout the series of **2**-Zn imidazole complexes (Table 4). Assuming that solid-state and solution structures correlate quite well in this series, it should be pointed out that the coordination of ImH or 2-MeBzImH induces a very similar red shift of **2**-Zn Soret and Q-bands. This suggests that distortion does not have a strong effect on the absorption maxima in this series of inclusion complexes, despite the various types and various amplitudes of distortions observed.[27]

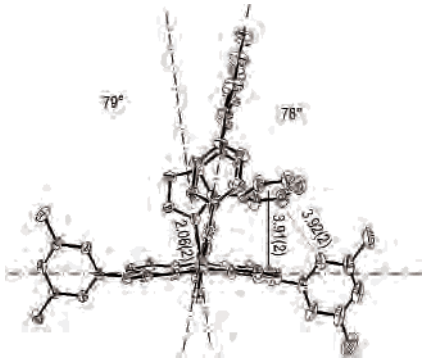

Figure 6. Side view of the distorted 2-PhImH⊂**2**-Zn inclusion complex.

Finally, in the case of 2-PhImH⊂**2**-Zn, the distortions observed in both the substrate and the receptor are introduced in the structure to preserve interactions already observed in the absence of the xylyl substituents, for 2-PhImH⊂**1**-Zn (Figure 6). The dihedral angle of 19.2° between the mean plane of the porphyrin and the phenyl substituent on the imidazole is larger than in the case of receptor **1**-Zn, but stacking of the these two aromatic moieties is still favored.

(27) There is currently a controversy concerning the origins of red-shifted optical spectra in nonplanar porphyrins; see for example: (a) Parusel, A. B. J.; Wondimagegn, T.; Ghosh, A. *J. Am. Chem. Soc.* **2000**, *122*, 6371. (b) Wertsching, A. K.; Koch, A. S.; DiMagno, S. G. *J. Am. Chem. Soc.* **2001**, *123*, 3932. (c) Ryeng, H.; Ghosh, A. *J. Am. Chem. Soc.* **2002**, *124*, 8099.

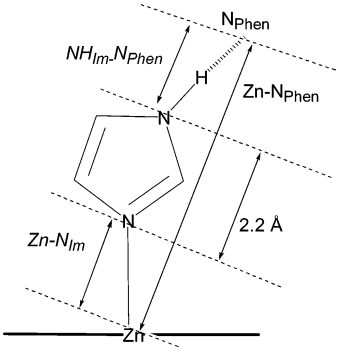

Figure 7. Rough estimation of the adequacy of the substrate/receptor.

An additional CH$-\pi$ interaction is observed with a distance of 3.92(2) Å displayed in Figure 6, between the centroid generated on the 2-phenyl and the xylyl aromatic proton in the *ortho* position on the distal side. This additional CH$-\pi$ interaction can explain the twist, and it emphasizes how the system generates a stabilizing interaction to compensate for the energy cost due to the larger dihedral angle between the stacked porphyrinic and phenyl rings. Stronger CH$-\pi$ interactions also contribute to the global stability of the inclusion complex with distances of 3.73(2) and 3.38(2) Å between the *ortho* CH of the phenyl substituent and a centroid generated on each spacer of the Phen strap.

A global estimation of the adjustments made by the receptor to accommodate the various substrates may be performed using the distances measured along the longitudinal axis of the cavity. Distances collected in Table 4 are identified in Figure 7 and show that a simple estimation of the space remaining for the substrate in each receptor can be made by subtracting projections of both the Zn$-$N$_{Im}$ coordination bond and the averaged NH$_{Im}-$N$_{Phen}$ distance (corresponding to the H-bond) along the axis connecting the zinc atom and the Phen nitrogen (Zn$-$N$_{Phen}$). From this estimation, it is reasonable to compare the space left for the substrate and the theoretical space needed for a perfect fit of the substrate in the receptor which is roughly 2.2 $\pm$ 0.1 Å, depending on the substitution of the imidazole ring.

From Table 4 data, the adequacy of the space available for ImHs insertion and the N---N distance in free imidazoles favors the formation of inclusion complexes in most cases. As shown in all side views of complexes, the tilt of the phenanthroline strap over the porphyrin plane, already observed in the structure of the free base,[17] decreases for a bulkier substitution in the 2 position of the imidazole. When bulk is introduced on the opposite side of the imidazole (positions 4 and 5), the tilt of the phenanthroline strap is not required for the insertion of ImH in the pocket. Instead, the distortion affects the porphyrin ring as demonstrated by the structure of 2-MeBzImH$\subset$**2**-Zn in Figure 5.

It should be noted that the poorest fit is observed for the unsubstituted imidazole ImH and that, for the corresponding inclusion complex ImH$\subset$**1**-Zn, the largest tilt of the Phen strap over the porphyrin ring is observed.[19] Of all the substrates, ImH and 2-MeBzImH are the only substrates for which fast exchange is observed in solution by ^{1}H NMR. Although this exchange is easily understandable for the bulkier substrate 2-MeBzImH, in the case of ImH no explanation other than a poor fit was valid, considering the very small geometrical differences observed in comparison to the structure of the free receptor **1**-Zn.[17]

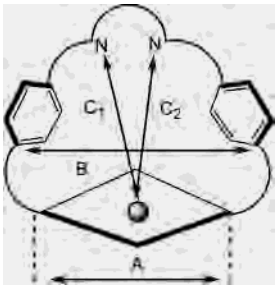

Figure 8. Longitudinal and lateral distortions of the Phen pocket.

Additional information is provided by the lateral distortions observed in the receptor for which significant distances identified in Figure 8 are listed in Table 5. When compared to the free base **1** that displays distances A and B of 7.01(3) and 9.70(2) Å, respectively,[17] imidazole complexation provokes a widening of the cavity defined by the spacers, as A is nearly constant (6.94 Å) and B is clearly increased to 10.47 Å in the structure of ImH$\subset$**1**-Zn.

It should be noted that the shortest B distance (9.26 Å) is observed for the inclusion of 2-MeBzImH in **2**-Zn, thus allowing maximum overlap between the aromatic walls of the cavity and the substrate. The variations in the width of the cavity seem to be directly correlated to the electron-rich character of the substrate, most probably to maximize the lipophilic interactions between the substrate and the receptor.

The more electron rich the imidazole is, the smaller the width of the Phen pocket. For bulkier substrates, this lateral shrinking permits a deeper penetration of the guest in the host and prevents a too drastic elongation of the H-bonds, thus compensating for the energy lost in the distortion of the porphyrin plane, as is the case for 2-MeBzImH$\subset$**2**-Zn. The receptor adjusts to allow guest insertion within the strap with changes that cost only a minimum of energy to the system. Ruffling of the porphyrin macrocycle allows the imidazole nucleus to enter deeper within the phenanthroline pocket, to preserve the overlap between the porphyrin electronic density and the phenyl substituent of the substrate, thus maintaining stabilizing $\pi-\pi$ interactions.

Conclusion and Perspectives

The phenanthroline-strapped receptors described in this paper display "induced fit" related distortions to accommodate bulky substrates on the hindered face of a zinc porphyrin. The binding site is selected on the basis of a strong metal to ligand coordination interaction that is finely tuned by establishing a bifurcated hydrogen bond, with a final adjustment achieved via weak interactions. Four basic distortions are observed at different levels: the porphyrin ring distortion; the longitudinal cavity distortion; the strap tilt above the plane of the porphyrin; the deviation of the Zn$-$N$_{imidazole}$ bond versus the normal to the porphyrin mean plane. The porphyrin ring distortion is related to the steric hindrance in the 4 and 5 positions of the imidazole. The tilt

Table 5. Lateral and Longitudinal Distortions in the Inclusion Complexes in the Solid State

param	**ImH**⊂**1**-Zn[a]	**2-MeImH**⊂1-Zn[a]	**2-PhImH**⊂1-Zn[b]	**2-MeImH**⊂2-Zn[b]	**2-MeBzImH**⊂2-Zn[b]	**2-PhImH**⊂2-Zn[b]
dist A (Å)	6.94	6.75	6.86	6.88	6.81	6.83
dist B (Å)	10.47	9.36	9.43	9.52	9.26	9.36
av C1, C2 (Å)	6.37	6.74	6.76	6.57	6.75	6.74

[a] Reference 19. [b] This work. A: distance between opposite *meso* carbons (C5 and C15) bearing the strap. B: distance between the extremities of the phenyl spacer. C_1 and C_2: distances between Zn and the Phen nitrogen atoms.

of the strap is allowed when no substituent is present in the 2 position of the imidazole. The deviation of the $Zn-N_{imidazole}$ from the normal to the porphyrin plane and the longitudinal cavity distortion are observed, if one or both of the previous adjustments are precluded or insufficient. These studies demonstrate how small geometric adjustments may be performed by initially rigid structures in order to produce energetically optimized supramolecular complexes. This very strong imidazole binding implies that if the coordination site of these Phen-strapped porphyrins is to be reserved exclusively for exogenic ligands, the use of *N*-alkylimidazoles as axial bases is a sin equa non condition. Detailed studies concerning the thermodynamics and kinetics of axial base ligation in these receptors need to be performed to assess, in particular, entropic and enthalpic contributions to this highly selective binding. Zinc(II) and iron(III/II) complexes are currently being studied by electrochemistry to determine how controlled small geometric variations influence the redox properties of heme and analogues. These results demonstrate that the synthetic availability of phenanthroline-strapped porphyrin **1** may be considered as a versatile starting material to easily access more elaborate superstructured porphyrins. Further functionalization of the porphyrinic core with "built-in" proximal ligands for iron(III/II) is currently in progress, as well as the construction of self-assembled photodyads through imidazole binding.[28]

Acknowledgment. The CNRS is gratefully acknowledged for financial support (Special Grant PCV 98-081), and D.P. thanks the French Government for an EGIDE postdoctoral fellowship.

Supporting Information Available: Experimental details for the synthesis of **2**-Zn, UV−vis titration of **1**-Zn with ImH, ^{1}H NMR titrations for **1**-Zn with 2-PhImH and 2-MeImH and for **2**-Zn with 2-PhImH and 2-MeBzImH, ROESY of 2-MeImH⊂**1**-Zn, NOESY of 2-MeImH⊂**2**-Zn, and ORTEP plots and atom numbering for 2-MeImH⊂**2**-Zn, **2**-PhImH⊂**1**-Zn, 2-PhImH⊂**2**-Zn, and 2-MeBzImH⊂**2**-Zn. This material is available free of charge via the Internet at http://pubs.acs.org.

IC0341643

(28) Wytko, J. A.; Paul, D.; Koepf, M.; Weiss, J. *Inorg. Chem.* **2002**, *41*, 3699.